JCTC Journal of Chemical Theory and Computation

Mechanism for the Substitution of an Aqua Ligand of $UO_2(OH_2)_5^{2+}$ by Chloride

François P. Rotzinger*

Institut des Sciences et Ingénierie Chimiques (ISIC), Ecole Polytechnique Fédérale de Lausanne (EPFL), Station 6, CH-1015 Lausanne, Switzerland

Received April 16, 2008

Abstract: Geometry and energy of the reactant ($UO_2(OH_2)_5 \cdot Cl^+$), the transition state ($UO_2(OH_2)_5 \cdots Cl^{+\ \ddagger}$), and the product ($UO_2Cl(OH_2)_4 \cdot OH_2^+$) of the title reaction have been computed with complete active space SCF (geometries and vibrational frequencies) and multiconfiguration quasi-degenerate second-order perturbation theory (total energies). Hydration was treated using the polarizable continuum model. The two investigated active spaces, (12/11) and (12/12), produce the same results. In contrast to the water exchange reaction on $UO_2(OH_2)_5^{2+}$, which proceeds via the associative (A) mechanism (which is a two step reaction involving an intermediate with an increased coordination number, $UO_2(OH_2)_6^{2+}$), water substitution by chloride follows the associative interchange (I_a) mechanism (which does not proceed via any intermediate). In this case, structure and imaginary mode of the transition state are not straightforward criteria for the attribution of the substitution mechanism, since they are both typical for the A pathway. The I_a mechanism was derived from the computed intrinsic reaction coordinate, which showed that no intermediate (for example $UO_2Cl(OH_2)_5^+$) exists as a local minimum on the potential energy surface. The activation free enthalpy is 31 kJ mol^{-1}. As for the water exchange reaction, the dissociative mechanism is unlikely to operate because of its higher free activation enthalpy (by ≈25 kJ mol^{-1}).

Introduction

The activation enthalpy ($\Delta H^{\ddagger}$) and free enthalpy ($\Delta G^{\ddagger}$) of the water exchange reaction 1 on the uranyl(VI) aqua ion have been measured with variable-temperature ^{17}O NMR techniques.[1]

$$UO_2(OH_2)_5^{2+} + H_2\mathbf{O} \rightarrow UO_2(\mathbf{O}H_2)(OH_2)_4^{2+} + H_2O \quad (1)$$

Substitution mechanisms are classified[2] as associative (A), dissociative (D), or concerted (I), whereby the concerted mechanism might have associative or dissociative character, which is denoted as I_a or I_d, respectively. The A and the D mechanisms proceed via intermediates with an increased or reduced coordination number, whereas the concerted pathways (I_a, I, or I_d) do not involve any intermediate. According to recent ab initio and DFT computations, the associative (A) mechanism is favored over the dissociative (D) mechanism by a rather modest energy of ≈15−25 kJ mol^{-1}.[3,4] Criteria for the distinction of the concerted (I_a) from the stepwise (A) substitution mechanism were presented.[3] The lifetime of the intermediate $UO_2(OH_2)_6^{2+}$ was estimated as ≈1−6 ps.[3]

In this article, the substitution of an aqua ligand of the uranyl(VI) aqua ion by chloride (reaction 2) was investigated using the same ab initio techniques as for reaction 1.[3]

$$UO_2(OH_2)_5^{2+} + Cl^- \rightarrow UO_2Cl(OH_2)_4^+ + H_2O \quad (2)$$

Static electron correlation was treated with complete active space SCF (CAS-SCF) and multiconfiguration quasi-degenerate second-order perturbation theory (MCQDPT2)[5,6] on the basis of the previously used (12/11) active space involving 12 electrons in 11 molecular orbitals (MOs) and a larger (12/12) active space used in recent studies of Hagberg et al.[7] and van Besien et al.[8] The computational methods, together with the approximations and limitations, are the same as in the previous study[3] and will not be reiterated.

* Corresponding author e-mail: francois.rotzinger@epfl.ch.

10.1021/ct8001305 CCC: $40.75 © 2008 American Chemical Society
Published on Web 09/12/2008

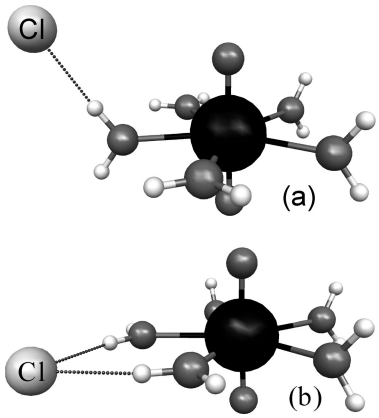

Figure 1. Perspective view of the reactant ion-pair $UO_2(OH_2)_5 \cdot Cl^+$ (CAS-SCF(12/11)-PCM geometry): (a) less stable isomer and (b) stable isomer.

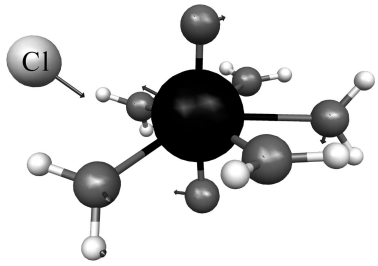

Figure 2. Perspective view and imaginary mode (55.6i cm^{-1}) of the transition state $UO_2(OH_2)_5 \cdots Cl^{+\ \ddagger}$ (CAS-SCF(12/11)-PCM geometry).

For reaction 2, no kinetic data are available, but its stability constant (K_{Cl}) has been estimated in several studies.[9−13] In an X-ray absorption fine structure (XAFS) spectroscopic study,[9] K_{Cl} was determined as ≈0.2−0.3 M^{-1} (25 °C). According to other work,[9−12] cited in the XAFS article, K_{Cl} is also smaller than 1 M^{-1}, 0.7−0.9 M^{-1}. In contrast, the dissociation constant determined spectroscopically by Hefley and Amis[13] is 2.28 × 10^{-2} M (in water at 25 °C and I = 1.238 M), from which K_{Cl} = 43.9 M^{-1} is derived.

Computational Details

All of the calculations were performed using the GAMESS[14] programs. For uranium, the relativistic effective core potential (ECP) basis set of Hay and Martin[15] was used, in which the 1s - 5s, 2p - 5p, 3d - 5d, and 4f shells are included in the relativistic core, and the 6s, 7s, 6p, 7p, 6d, and 5f shells are represented by a (10s, 8p, 2d, 4f) basis set contracted to [3s, 3p, 2d, 2f]. For O and H, the 6−31G(d) basis set[16,17] was used (α_d = 1.20[18]), and for chlorine, the ECP basis set of Stevens et al.[19] supplemented with a d polarization function (α_d = 0.65[18]) was used. Figures 1, 2, and 4 were generated with MacMolPlt.[20]

The Hessians, the total energies, and the thermodynamic variables ($\Delta H^{\ddagger}$, ΔH, $\Delta S^{\ddagger}$, ΔS, $\Delta G^{\ddagger}$, and ΔG) at 25 °C were computed as described.[3] Hydration was treated using the polarizable continuum model (PCM)[21,22] as reported previously.[3] Geometries and vibrational frequencies were calculated at the CAS-SCF(12/11)-PCM and CAS-SCF(12/12)-PCM levels, and the total energies were computed with

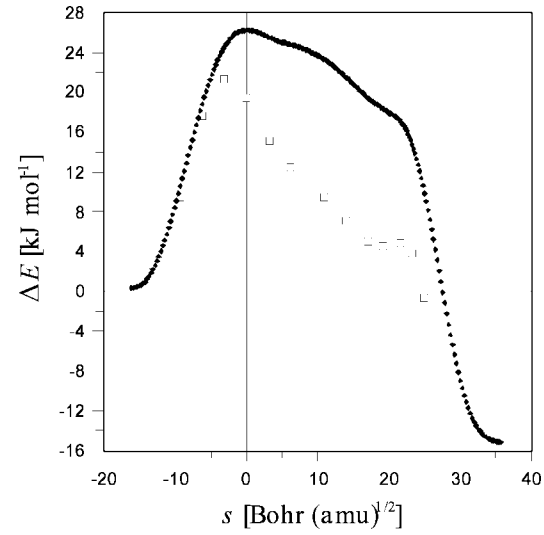

Figure 3. Intrinsic reaction coordinate of reaction 4 (CAS-SCF(12/11)-PCM geometries: CAS-SCF(12/11)-PCM energies (♦) and MCQDPT2(12/11)-PCM energies (□).

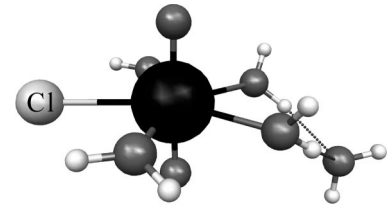

Figure 4. Perspective view of the product $UO_2Cl(OH_2)_4 \cdot OH_2^+$ (CAS-SCF(12/11)-PCM geometry).

MCQDPT2(12/11)-PCM and MCQDPT2(12/12)-PCM.[3] The atomic coordinates of the investigated species are given in Tables S1−S4 (Supporting Information).

The transition state was located by maximizing the energy for the imaginary U···Cl stretching mode via Eigen-mode following, whereby along all of the other modes, the energy was minimized. The intrinsic reaction coordinate (IRC), which is the steepest descent path or the minimum energy path, was computed on the basis of the second-order Gonzalez-Schlegel method.[23]

Results

Active Space for the CAS-SCF and MCQDPT2 Calculations and Model for Reaction 2. Configuration interaction singles-doubles CISD calculations on $UO_2(OH_2)_5^{2+}$ indicated that static electron correlation should be treated at least via a (12/11) active space,[24] which has been used for the study of reaction 1.[3] Preferably, active spaces are chosen to be composed of the corresponding bonding and antibonding pairs of MOs, which gives rise to the same number of electrons and orbitals for closed shell systems. This principle has been applied in the CASPT2(12/12) studies of Hagberg et al.[7] and van Besien et al.[8] In this study, it will be shown that there is no loss of accuracy, when the σ^*(U═O) MO with a much lower occupation[3] than the other antibonding σ^*(U═O) MO is excluded from the active space.

For the investigation of reaction 2 with quantum chemical methods, (2) is decomposed into reaction 3 describing the

Table 1. Selected Bond Lengths (Å) of the Uranyl(VI) Complexes Involved in Reaction *2*

	active space	U=O	U−O	U···O	U−Cl or U···Cl	H···Cl or H···O
$UO_2(OH_2)_5 \cdot Cl^+$ [a]	(12/11)	1.761, 1.762	2.460, 2.519, 2.499, 2.498, 2.518		4.884	2.127
$UO_2(OH_2)_5 \cdot Cl^+$ [b]	(12/11)	1.762, 1.762	2.502, 2.502, 2.504, 2.499, 2.504		4.883	2.237, 2.239
$UO_2(OH_2)_5 \cdot Cl^+$ [b]	(12/12)	1.771, 1.771	2.502, 2.502, 2.505, 2.499, 2.504		4.884	2.236, 2.239
$UO_2(OH_2)_5 \cdots Cl^{+\ddagger}$	(12/11)	1.758, 1.761	2.572, 2.572, 2.549, 2.541, 2.550		3.283	2.455, 2.455
$UO_2(OH_2)_5 \cdots Cl^{+\ddagger}$	(12/12)	1.767, 1.770	2.571, 2.569, 2.548, 2.539, 2.549		3.290	2.458, 2.457
$UO_2Cl(OH_2)_4 \cdot OH_2^+$	(12/11)	1.763, 1.763	2.524, 2.524, 2.512, 2.512	4.143	2.820	1.869, 1.873
$UO_2Cl(OH_2)_4 \cdot OH_2^+$	(12/12)	1.772, 1.772	2.525, 2.525, 2.512, 2.513	4.152	2.819	1.870, 1.870

[a] Less stable isomer. [b] Stable isomer.

Table 2. Thermodynamic Activation and Reaction Energies and Entropies

active space	$\Delta E^{\ddagger}$ (ΔE) [kJ mol^{-1}]	$\Delta H^{\ddagger}$ (ΔH) [kJ mol^{-1}]	$\Delta S^{\ddagger}$ (ΔS) [J K^{-1} mol^{-1}]	$\Delta G^{\ddagger}$ (ΔG) [kJ mol^{-1}]
		Reaction 4, I_a Mechanism		
(12/11)	19.1 (−24.9)	18.4 (−23.3)	−42.3 (−25.7)	31.0 (−15.7)
(12/12)	19.9 (−23.7)	19.2 (−22.2)	−43.0 (−24.1)	32.0 (−15.0)
		Reaction 1, A Mechanism[a]		
(12/11)	25.6 (20.5)[b]	22.9 (20.2)[b]	−23.4 (−2.4)[b]	29.9 (20.9)[b]
		Reaction 1, D (or I_d) Mechanism[a]		
(12/11)	52.6 (47.9)[c]	50.0 (48.7)[c]	−24.0 (−14.9)[c]	57.1 (53.2)[c]

[a] Reference 3. [b] Intermediate $UO_2(OH_2)_6^{2+}$. [c] Intermediate $UO_2(OH_2)_4 \cdot OH_2^{2+}$.

formation of the ion-pair $UO_2(OH_2)_5 \cdot Cl^+$ ($K_{IP,Cl}$) and reaction 4 representing the substitution of an aqua ligand by Cl^- (K_{Cl}').

$$UO_2(OH_2)_5^{2+} + Cl^- \rightarrow UO_2(OH_2)_5 \cdot Cl^+ \quad (3)$$

$$UO_2(OH_2)_5 \cdot Cl^+ \rightarrow UO_2(OH_2)_5 \cdots Cl^{+\ddagger} \rightarrow UO_2Cl(OH_2)_4 \cdot OH_2^+ \quad (4)$$

The ion-pair formation constant ($K_{IP,Cl}$) can be estimated on the basis of the Fuoss equation;[25] it amounts to 0.84 M^{-1} at 25 °C and $I = 1.238$ M^{-1} (the U···Cl distance is 4.88 Å for both isomers of $UO_2(OH_2)_5 \cdot Cl^+$, Table 1). It should be noted that the Fuoss equation takes into account entropy effects approximately. The thermodynamic values and the equilibrium constant (K_{Cl}') for reaction 4 were determined via quantum chemical calculations. Thus, the equilibrium constant for reaction 2, K_{Cl}, is available from eq 5.

$$K_{Cl} = K_{IP,Cl} K_{Cl}' \quad (5)$$

Reactant $UO_2(OH_2)_5 \cdot Cl^+$. For this ion-pair, there are two isomers: in the less stable one, the chloride ion forms a single hydrogen bond with $UO_2(OH_2)_5^{2+}$ (Figure 1a), and in the more stable isomer, Cl^- forms two hydrogen bonds with the uranyl(VI) cation (Figure 1b). The MCQDPT2(12/11)-PCM energy difference is 13.0 kJ mol^{-1}, and the free enthalpy difference is virtually equal, 12.8 kJ mol^{-1}. Selected bond lengths of all investigated uranyl(VI) complexes are reported in Table 1. The less stable isomer will not be considered further, since activation and reaction energies have to be based on the global minimum. The MCQDPT2(12/11)-PCM and MCQDPT2(12/12)-PCM energies together with the pertinent thermodynamic values ($\Delta H^{\ddagger}$, ΔH, $\Delta S^{\ddagger}$, ΔS, $\Delta G^{\ddagger}$, and ΔG) for reaction 4 are summarized in Table 2.

The increase of the active space from (12/11) to (12/12) leads to an elongation of the U=O bonds by 0.009 Å for all species (Table 1). The activation or reaction energies and entropies are equal within ≈1 kJ mol^{-1} and ≤2 J K^{-1} mol^{-1}, respectively (Table 2).

Transition State $UO_2(OH_2)_5 \cdots Cl^{+\ddagger}$. Its geometry, involving an elongated U···Cl bond, but U−O bonds as in the reactant (Table 1), would suggest that this is a transition state for the A mechanism (as that for reaction 1[3]). The H_2O ligand trans to the entering Cl^- ion will leave, although it has the shortest U−O bond (which will be referred to as U−O_{trans}). The imaginary mode (Figure 2) represents the entry of the Cl^- ion into the first coordination sphere and a small out-of-plane motion of the trans H_2O ligand. Thus, also the imaginary mode might suggest the A mechanism. However, this substitution reaction 4 proceeds via the I_a pathway, since intermediates are absent from the computed (CAS-SCF(12/11)-PCM level) intrinsic reaction coordinate (IRC) *s* (Figure 3).

The transition state is formed via a common reaction coordinate (Figure 3, negative *s* values), which represents the shortening of the U···Cl bond that occurs concerted with the rearrangement of the H_2O ligands. The IRC calculation (started from the transition state) yields the stable reactant isomer. This proves that the transition state is indeed formed from the reactant in the global minimum.

Product formation (Figure 3, positive *s* values) involves two stages, shortening of the U···Cl bond followed by the elongation of the U−O_{trans} bond. In the range of $s \approx 0-20$ Bohr (amu)$^{1/2}$, there are several inflection points, and the energy does not diminish strongly at the CAS-SCF(12/11)-PCM level (Table 3). Afterward, at $s \gtrsim 22$ Bohr (amu)$^{1/2}$, the U−O_{trans} bond length increases strongly during the steep energy drop leading to the product. In the first stage, the U···Cl bond shortens rapidly to ≈3 Å (at $s \approx 0-6$ Bohr (amu)$^{1/2}$), while the U−O_{trans} bond is elongated only slightly (up to $s \approx 11$ Bohr (amu)$^{1/2}$). In the range of $s \approx 6-11$ Bohr (amu)$^{1/2}$ both, the U−Cl and the U−O_{trans} bonds, change only marginally, and their sum is minimal. The species in this *s* range has a geometry that would be typical for a $UO_2Cl(OH_2)_5^+$ intermediate. Since, however, in this *s* range of ≈6−11 Bohr (amu)$^{1/2}$, no local minimum is present on the potential energy surface (PES), an intermediate for

Table 3. Bond Parameters That Change in a Pronounced Manner during the Transformation of the Transition State into the Product

s [Bohr (amu)$^{1/2}$]	U−Cl [Å]	U−O_{trans} [Å]	∠(O=U−O_{trans}) [°]
0[a]	3.283	2.541	86.5
6.225	3.024	2.591	83.8
10.944	2.969	2.637	78.5
16.998	2.914	2.726	71.3
21.513	2.876	2.940	65.5

[a] Transition state $UO_2(OH_2)_5\cdots Cl^{+\ddagger}$.

the A mechanism does not exist. In the present case, the local minimum is absent most likely, since the reaction is asymmetric (H_2O is substituted by Cl^-), and since the free reaction enthalpy is negative.

The IRC represents the minimum energy pathway. Thus, the substitution of the H_2O ligand trans to the entering Cl^- is the most facile process. The elimination of one of the other four H_2O ligands does not correspond to a minimum energy path, and, hence, such processes are unlikely to be competitive with the elimination of the trans H_2O ligand. If another isomer for the transition state $UO_2(OH_2)_5\cdots Cl^{+\ddagger}$ existed, it would not be possible to exclude that a pathway giving rise to the elimination of one of the nontrans H_2O ligands would take place. However, within the present model, there is only one isomer for the transition state because of the high symmetry of the $UO_2(OH_2)_5^{2+}$ ion.

In the determination of the CAS-SCF(12/11)-PCM geometries and frequencies, dynamic electron correlation was neglected. Therefore, these data are approximate. The MCQDPT2(12/11)-PCM technique produces the most accurate total energies with minimal computational efforts for the present system, but it should be remembered that they are based on approximate geometries. Thus, the difference between the MCQDPT2(12/11)-PCM and the CAS-SCF(12/11)-PCM energies (Figure 3) is due to dynamic electron correlation. At $s \approx 18.5$ Bohr (amu)$^{1/2}$, there is a very shallow local minimum on the MCQDPT2(12/11)-PCM PES. Its depth amounts to <0.3 kJ mol^{-1} which means that the lifetime (τ_I) of this intermediate would be <0.2 ps. Since τ_I is smaller than the duration of the vibration (τ_{vib}) leading to the product ($\tau_{vib} \approx 0.3-0.4$ ps[3]), this "intermediate" does not exhibit a significant lifetime, and, therefore, it is irrelevant for the reactivity and the reaction mechanism.[3] Hence, also on the basis of the MCQDPT2(12/11)-PCM energies, the I_a mechanism is attributed to reaction 4.

The imaginary mode (Figure 2) reflects the uncommon transition state structure: it describes the entry of the Cl^- ion without concerted elongation of the U−O_{trans} bond of the leaving ligand. For the I_a as well as the I and I_d mechanisms, the imaginary mode represents usually the *concerted* motions of the entering and leaving ligands.[26] The U−O_{trans} bond stretching component is missing because in the transition state, this bond is not weakened; this process takes place later, at $s \gtrsim 17$ Bohr (amu)$^{1/2}$.

The thermodynamic activation free enthalpy of reaction 4 for the I_a pathway is virtually equal to that of reaction 1 via the A mechanism (Table 2).

Product $UO_2Cl(OH_2)_4\cdot OH_2^+$. It exhibits a U−Cl bond of 2.82 Å (Table 1 and Figure 4), which is too long by 0.1 Å compared with the experimental value of 2.71−2.72 Å.[9] As pointed out previously,[3,24] this error arises from the neglect of dynamic electron correlation. The product is more stable by 15 kJ mol^{-1} than the reactant ion-pair (Table 2).

Discussion

Comparison with Experimental Data. As already mentioned in the Introduction, the experimental data[9−13] for K_{Cl} are controversial. On the basis of Hefley and Amis's K_{Cl} value of 43.9 M^{-1} (in water at 25 °C and $I = 1.238$ M),[13] and $K_{IP,Cl} = 0.84$ M^{-1} based on the Fuoss equation[25] (25 °C and $I = 1.238$ M), $K_{Cl}' = 52.3$ is estimated. ΔG based on this K_{Cl}' value is −9.8 kJ mol^{-1}, which agrees well with ΔG computed for reaction 4 (Table 2). According to the other experimental data,[9−12] ΔG for (4) would be slightly positive ($\approx$2 kJ mol^{-1}). All of the experimental data lie within the computational accuracy, which is $\leqslant$10−15 kJ mol^{-1}. The approximations and limitations of the model and the computational methods have already been discussed.[3]

Comparison with Other Computed Data. Very recently, Bühl et al.[27] studied the stability of chloro complexes of $UO_2(OH_2)_5^{2+}$ as well as their coordination numbers with density functional theory (DFT). For reaction 2, they obtained $\Delta G = -27.2$ and −18.4 kJ mol^{-1}, respectively, using the BLYP and B3LYP functionals and PCM hydration. On the basis of Car−Parrinello MD simulations based on the BLYP functional, they computed $\Delta A = 9.6$ kJ mol^{-1}. Apart from the BLYP-PCM result, their computed data agree with experiment and the present MCQDPT2-PCM results.

The B3LYP geometries of the $UO_2(OH_2)_5^{2+}$ ion in aqueous solution, for example,[3] are more accurate than the CAS-SCF geometries, but the uranyl(VI)−ligand bond lengths remain too long in comparison with experiment.[3,27] In spite of the worse geometries of CAS-SCF compared with B3LYP, high-level ab initio energies are more accurate than DFT energies.[3,28] The above-discussed DFT calculations[3,27,28] were performed with commonly used functionals. It will be interesting to see computational results on such systems which are realized with, for example, the very recent novel and promising functionals developed by Zhao and Truhlar.[29]

Substitution Mechanism of Reaction 4. The water exchange reaction 1 proceeds most likely via the A mechanism, which involves the $UO_2(OH_2)_6^{2+}$ intermediate.[3] Since its lifetime (τ_I) is short, only slightly longer than the duration of the vibration (τ_{vib}) leading to the product, the attribution of the A mechanism cannot be definitive.[3] It was shown in this Results section that structure and imaginary mode (Table 1 and Figure 2) of the transition state for reaction 4 are typical for the A mechanism but that due to the absence of any intermediate on the intrinsic reaction coordinate (Figure 3) reaction 4 proceeds via the I_a mechanism. As shown in the Results section, this substitution reaction proceeds in two steps: the first one is the formation of a $UO_2Cl(OH_2)_5^+$ species via shortening of the U$\cdots$Cl bond after the transition state. In the second step, the U−O_{trans} bond is broken, which leads to the product. Since there is no local minimum on

this PES (Figure 3), this two-stage process has to be classified as I_a. This example shows that structure and imaginary mode of the transition state are not sufficient criteria for the determination of the reaction mechanism; it is necessary to find all of the stationary points on the PES between the reactant and the product. Compared with the water exchange reaction 1 exhibiting H_2O as entering ligand, the Cl^- ion causes a change of the mechanism from A to I_a, most likely because of the asymmetry and the exergonicity of reaction 4.

The activation energy for the D mechanism is (by definition) independent of the entering ligand. In both reactions 1 and 4, a H_2O ligand is eliminated from the $UO_2(OH_2)_5^{2+}$ cation. Hence, the activation energy for water substitution *via the D mechanism* would be equal for these two reactions. However, a *small* difference in activation energies arising from differences in the environment of the cation, Cl^- being present in the second coordination sphere for (4) and absent for (1), can be expected. This difference will never amount to the sizable I_a-D activation energy difference of $\approx$25 kJ mol^{-1}. The conclusion that reaction 4 follows the I_a mechanism is safe. For (1) and (4), the activation free enthalpies for the D pathway would be approximately equal and higher by $\approx$25 kJ mol^{-1} than those for the A and I_a mechanisms (Table 2). Thus, as for reaction 1, the dissociative mechanism is unfavorable for (4).

The hydration of the $Cr(NH_3)_5Cl^{2+}$ complex follows the I_a mechanism,[30,31] whereby the corresponding transition state structure is typical for the I_a mechanism, although this reaction is also asymmetric: the bonds of both ligands, Cl^- and H_2O, which are involved in the substitution reaction, are longer than in the reactant or the product. This is the reason why such transition states are denoted as $Cr(NH_3)_5\cdots(Cl)(OH_2)^{2+\ddagger}$, for example. The imaginary mode describes the *concerted* formation and breaking of the bonds of the entering and leaving ligands, respectively.[26] Compared with such usual transition states for the I_a (and I_d) mechanism,[26] the transition state of (4) is atypical, since it does not exhibit two elongated bonds. A typical transition state for I_a (with two elongated bonds) would be denoted as $UO_2(OH_2)_4\cdots(Cl)(OH_2)^{+\ddagger}$. Hence, because of the absence of an elongated U$\cdots$O bond, this I_a transition state is described as $UO_2(OH_2)_5\cdots Cl^{+\ddagger}$.

Note Added after ASAP Publication. This article was released ASAP on September 12, 2008, with minor errors in the first column of Table 1. The correct version was posted on September 20, 2008.

Supporting Information Available: Atomic coordinates of the species involved in eq 4 (CAS-SCF(12/11)-PCM and CAS-SCF(12/12)-PCM geometries) (Tables S1−S4). This material is available free of charge via the Internet at http://pubs.acs.org.

References

(1) Farkas, I.; Bányai, I.; Szabó, Z.; Wahlgren, U.; Grenthe, I. *Inorg. Chem.* **2000**, *39*, 799.

(2) Merbach, A. E. *Pure Appl. Chem.* **1982**, *54*, 1479.

(3) (a) Rotzinger, F. P. *Chem. Eur. J.* **2007**, *13*, 800. (b) Corrigendum.

(4) Bühl, M.; Kabrede, H. *Inorg. Chem.* **2006**, *45*, 3834.

(5) Nakano, H. *J. Chem. Phys.* **1993**, *99*, 7983.

(6) Nakano, H. *Chem. Phys. Lett.* **1993**, *207*, 372.

(7) Hagberg, D.; Karlström, G.; Roos, B. O.; Gagliardi, L. *J. Am. Chem. Soc.* **2005**, *127*, 14250.

(8) Van Besien, E.; Pierloot, K.; Görller-Walrand, C. *Phys. Chem. Chem. Phys.* **2006**, *8*, 4311.

(9) Allen, P. G.; Bucher, J. J.; Shuh, D. K.; Edelstein, N. M.; Reich, T. *Inorg. Chem.* **1997**, *36*, 4676.

(10) Day, R. A.; Powers, R. M. *J. Am. Chem. Soc.* **1954**, *76*, 3895.

(11) Bednarczyk, L.; Fidelis, I. *J. Radioanal. Nucl. Chem.* **1978**, *45*, 325.

(12) Awasthi, S. P.; Sundaresan, M. *Indian J. Chem.* **1981**, *20A*, 378.

(13) Hefley, J. D.; Amis, E. S. *J. Phys. Chem.* **1960**, *64*, 870.

(14) (a) Schmidt, M. W.; Baldridge, K. K.; Boatz, J. A.; Elbert, S. T.; Gordon, M. S.; Jensen, J. H.; Koseki, S.; Matsunaga, N.; Nguyen, K. A.; Su, S. J.; Windus, T. L.; Dupuis, M.; Montgomery, J. A. *J. Comput. Chem.* **1993**, *14*, 1347. (b) Gordon, M. S.; Schmidt, M. W. In *Theory and Applications of Computational Chemistry, the first forty years*; Dykstra, C. E., Frenking, G., Kim, K. S., Scuseria, G. E., Eds.; Elsevier: Amsterdam, 2005; pp 1167−1189.

(15) Hay, P. J.; Martin, R. L. *J. Chem. Phys.* **1998**, *109*, 3875.

(16) Hehre, W. J.; Ditchfield, R.; Pople, J. A. *J. Chem. Phys.* **1972**, *56*, 2257.

(17) Ditchfield, R.; Hehre, W. J.; Pople, J. A. *J. Chem. Phys.* **1971**, *54*, 724.

(18) Schäfer, A.; Horn, H.; Ahlrichs, R. *J. Chem. Phys.* **1992**, *97*, 2571.

(19) Stevens, W. J.; Basch, H.; Krauss, M. *J. Chem. Phys.* **1984**, *81*, 6026.

(20) Bode, B. M.; Gordon, M. S. *J. Mol. Graphics Modell.* **1998**, *16*, 133.

(21) Tomasi, J. *Theor. Chem. Acc.* **2004**, *112*, 184.

(22) Tomasi, J.; Mennucci, B.; Cammi, R. *Chem. Rev.* **2005**, *105*, 2999.

(23) Gonzalez, C.; Schlegel, H. B. *J. Chem. Phys.* **1989**, *90*, 2154.

(24) Rotzinger, F. P. *Chem. Eur. J.* **2007**, *13*, 10298.

(25) Fuoss, R. M. *J. Am. Chem. Soc.* **1958**, *80*, 5059.

(26) Rotzinger, F. P. *Chem. Rev.* **2005**, *105*, 2003.

(27) Bühl, M.; Sieffert, N.; Golubnychiy, V.; Wipff, G. *J. Phys. Chem. A* **2008**, *112*, 2428.

(28) Rotzinger, F. P. *J. Phys. Chem. B* **2005**, *109*, 1510.

(29) Zhao, Y.; Truhlar, D. G. *Acc. Chem. Res.* **2008**, *41*, 157.

(30) Guastalla, G.; Swaddle, T. W. *Can. J. Chem.* **1973**, *51*, 821.

(31) Rotzinger, F. P. *Inorg. Chem.* **1999**, *38*, 5730.

CT8001305